

Ultrafast-Laser Manufacture of Radially Emitting Optical Fiber Diffusers for Medical Applications

Stephan Ströbl*,**, Christoph Vonach*, Johannes Gratt*, Matthias Domke*, Ronald Sroka**

* Vorarlberg University of Applied Sciences, Dornbirn, Austria

stephan.stroebl@fhv.at

** Laser-Forschungslabor, LIFE-Zentrum – Department of Urology, University Hospital Munich, Germany

Photodynamic Therapy (PDT) is a gentle method to treat cancer through irradiation by light. To guarantee a positive result from the treatment, a complete illumination of the treated malignant volume has to be reached. The technical challenge is to specifically decouple light from a wave guide, inserted into malignant regions. The aim of this study was to measure and simulate the radiation profile of radially emitting diffusers. An ultrafast laser system combined with a rotational axis was used to machine the distal end of optical fibers. Cylindrical and tapered shaped diffusers were produced. A low power diode laser ($\lambda = 670$ nm) was coupled into the fiber to determine the emission profile, which was measured via a camera setup. The measured emission profiles were simulated using a 2D-Matlab model and a 3D-LightTools model. The simulated and measured intensity profile along the cylindrical and the tapered fiber tip is characterized by an intensity maximum at the beginning, constant intensity in the middle, and exponentially decreasing intensity at the end. The studies indicate that fiber diffusers with tailored 3D radiation profile can be manufactured using ultrafast lasers. Further investigations have to be performed to adapt the simulations to the measured data.

DOI: 10.2961/jlmn.2019.01.0008

Keywords: ultrashort pulse, laser ablation, optical fiber, radial fiber diffuser, Monte Carlo method, raytracing, photodynamic therapy

1. Introduction

Interstitial Photodynamic Therapy (iPDT) is a low power radiation method to selectively treat brain cancer [1]. A drug (ALA – aminolevulinic acid) is administered per os to the patient, which induces an accumulation of protoporphyrine IX (PPIX), a photosensitive drug, selectively within the cancer cells, due to bypassing the regulation of the ferrochelatase, the last step in the heme-biosynthesis. When illuminating the photosensitive brain regions via a light wave guide with non-thermal light intensities at a certain wavelength (for PPIX: $\lambda = 635$ nm), the PPIX molecules become excited. When it relaxes to the ground level, the available energy can be transferred to the tissue oxygen, and a reactive singlet oxygen species is generated. The reactive oxygen species acts toxic towards the nearby cancer cells. Thereby, the tumor cells are eliminated selectively, while the healthy tissue remains untouched. [1-3]

For the iPDT optical fibers are used to deliver the light into the treated brain volume. The light has to be homogeneously decoupled from the fiber to guarantee uniform illumination of the treatment site [4-8]. Therefore, diffusers are affixed to the distal end of the fiber. Currently, the most common technical realization is to use scattering material (e.g. TiO_2) embedded in silicone, which is connected to the fiber tip. By varying the particle density of the scattering material along the diffuser length, the radiation profile can be changed. Although the diffuser technology undergoes permanent development, there is a loss of power and hence heat generation observable at the transition zone between the distal bare fiber end and the affixed diffuser tip. The generation of heat can damage the transition zone between fiber and diffuser tip. As the

development of heat is not desired for low power applications and may be critical to adjacent healthy tissue, different approaches were developed solving this limitation in the past years.

One approach targets on surface ablation directly on the light wave guide. For example, a CO_2 laser ($\lambda = 10,600$ nm) can be used to create a grid like structure on the fiber surface. Thereby, the surface gets roughened, leading to a disruption of total internal reflection, whereby the chance of photon decoupling from the fiber core is increased [9, 10]. However, the radiation profile could not be modified by varying the structural changes, as the method ablates quite roughly on the fiber surface. This can be attributed to the large focal spot of the CO_2 laser due to its emission wavelength of $\lambda = 10,600$ nm.

Using an excimer laser, the fiber tips could also be modified [11]. Focusing inside the fiber core, ablation through the whole fiber core was achieved. Due to its emission wavelength $\lambda = 248$ nm, a small focal spot could be achieved, which allowed for a drilling through the fiber core. Although a decoupling of laser light was achieved, the method didn't allow a reproducible manufacturing process of fiber diffusers so far.

The use of ultrafast-lasers with pulse durations in the range of femtoseconds allows a clean and reproducible targeting of the fiber core. The use of ultrafast-lasers can be split in two approaches. One targets at the surface ablation of the fiber core [15], the other one at internal modifications [12-14]. By focusing the laser beam inside the fiber core, the cladding remains untouched, whereas the material within the laser focus gets modified [16]. By delivering sufficient energy to a certain region, altering of the refractive index could be observed. The regions of modified refractive

indices act as scattering centers and disrupt the light guidance through the fiber. Thereby, light gets decoupled from the fiber. As the cladding around the fiber core is not targeted, the mechanical stability of the fiber remains even after modifying the core. [12-14]

An external structuring approach using an ultrafast-laser showed that it is possible to homogenize the emission profile of a diffuser by fabricating rectangular defects with varying geometry [15]. The geometry of each defect was determined by performing a two-dimensional ray tracing simulation with defects on one side of the fiber. The approach worked well for one sided defects but it has not been verified for three-dimensional radially emitting diffusers so far [15]. Therefore, a new fabrication method was developed, which allows to manufacture radially emitting fiber diffusers. The procedure is based on adding a rotational axis to the workbench of the ultrafast-laser, in which the fiber is fixed. In a first approach, two diffuser geometries were produced, a cylindrical and a tapered shaped one. The radiation profile of the produced fiber diffusers were measured using a camera setup and were compared to simulation data. To verify the measured radiation profiles, two different simulation approaches were used, a two-dimensional Monte-Carlo simulation (Matlab) and a ray tracing software (LightTools).

2. Materials & Methods

For this study two different diffuser geometries were fabricated using a laser processing machine (microSTRUCT vario, 3D-Micromac, Chemnitz, Germany) equipped with an ultrafast-laser system (Spirit, Spectra-Physics, Rankweil, Austria). The laser pulses were applied onto an optical fiber (E-6100-B, Dornier MedTech GmbH, Weßling, Germany). The fiber has a silica core with a diameter of 600 μm and a refractive index of $n_{\text{core}} = 1.46$. The core is surrounded by a polymer cladding with a thickness of 15 μm and a refractive index of $n_{\text{cladding}} = 1.37$. The core and cladding is surrounded by a polymer buffer, which enhances the mechanical stability of the fiber. However, to allow surface ablation on the fiber core, the polymer buffer had to be removed.

In order to ablate material from the cladding and the silica core effectively, specific laser parameter were chosen. The pulse duration of the laser system is $t_p = 380$ fs and the pulse repetition rate $f_{\text{rep}} = 200$ kHz. The output wavelength was set to $\lambda = 520$ nm. By using a long-focal-length objective ($f = 170$ mm), the radius of the focused beam was set to $\omega_0 = 6$ μm . The Rayleigh length of the beam was calculated to be $z_R = 217$ μm . To obtain maximal ablation efficiency, the laser fluence was set to $\Phi = 4 \text{ J/cm}^2$ by setting the emitted laser power to $P = 0.25 \text{ W}$ [17]. The scanning speed of the laser beam was set to $v = 1000 \text{ mm/s}$, leading to a pulse-to-pulse distance of 5 μm . In order to ablate areas of a width bigger than the beam width, the laser scanner has to scan over the intended area in parallel lines with a line spacing set to 5 μm . To obtain an ablation area of constant depth, the parallel lines were rotated after each scanning step. The depth of the ablated area is connected linearly to the number of scanning cycles [18].

The fabrication of radially emitting fiber diffusers requires the implementation of a rotation axis as the laser focus position is stationary and can only be varied in xy-direction. Therefore, the decoated fiber tip needs to be

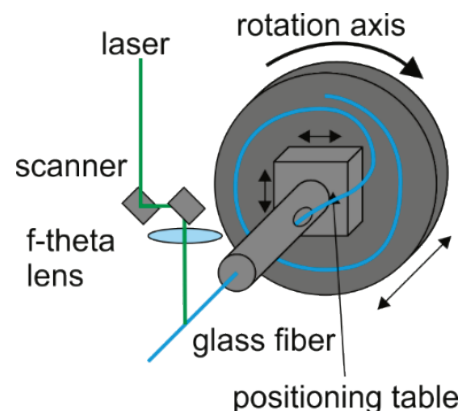


Fig. 1 Schematic setup of ultrafast-laser fiber processig with rotational axis.

tightly strapped to a rotation axis. The structure of the mount is schematically drawn in Fig. 1. In order to align the fiber surface to the focal plane of the laser, the fiber is mounted on a positioning table and a tiltable stage to adjust the fiber to the focal plane. After setting the rotational shift of the rotation stage to 9°, a cylindrical and a tapered shaped diffuser was fabricated. In Fig. 2a, a SEM image of a cylindrically processed fiber tip is shown. Fig. 2b shows a tapered fiber tip geometry with a diffuser length of 20 mm.

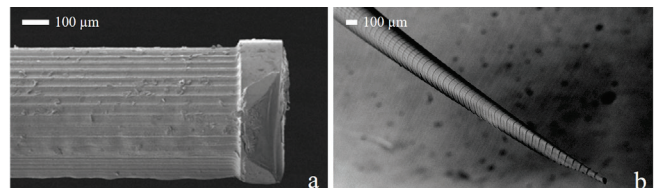


Fig. 2 SEM images (JSM-7100F, JEOL, Tokyo, Japan) of manufactured fiber tips. - a: cylindrical, b: tapered.

The radiation profile of the manufactured diffuser types was measured using a monochrome camera imaging system (DMK41AU02, TheImagingSource Europe GmbH, Bremen, Germany). The exposure time of the camera was set to 1/10000 s to avoid over-saturation of pixels. The light of a laser diode (LPM670, Thorlabs GmbH, Dachau, Germany) was coupled into the fiber using a lens ($f = 75$ mm). The output wavelength of the diode is $\lambda = 670$ nm with a maximum emission power of 5.5 mW. The camera objective was focused onto the fiber surface, which was positioned at a distance of 30 cm to the camera objective. To reduce background reflections, the mounting socket for the fiber diffuser was painted matt-black and the surrounding room light was switched off. The schematic camera setup to obtain the radiation profile of diffuse emitting fibers is illustrated in Fig. 3.

The recorded image is analyzed using an open access software (ImageJ, Bethesda, MA, USA). The software allows the measurement of pixel brightness along a path with a specific width. In order to reduce noise due to laser speckle effects, five consecutive pixel lines were selected and averaged. The surface brightness with its corresponding position along the diffuser were graphically visualized for the cylindrical and the tapered diffuser.

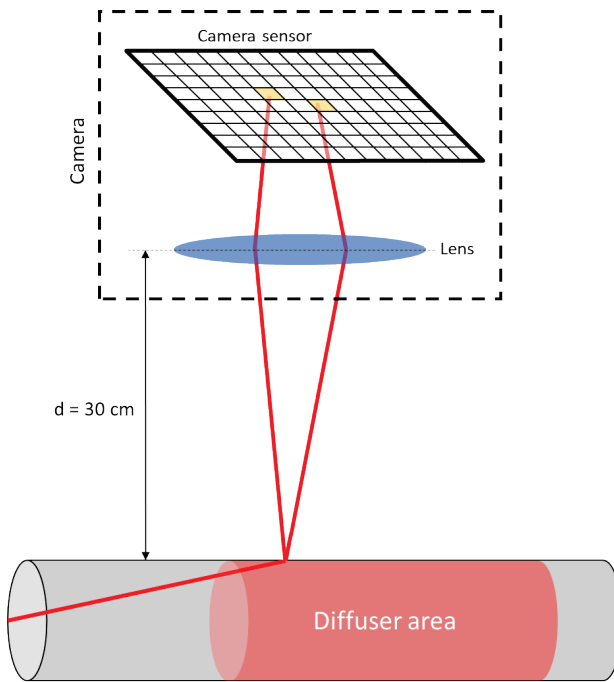


Fig. 3 Schematic measurement setup to obtain the radiation profile of a fiber diffuser.

In order to evaluate for the power irradiated to a certain tissue volume, a correction has to be applied to the tapered diffuser. As the surface area per diffuser length reduces gradually over the diffuser length, a factor has to be added to the measured intensity values. Therefore, the measured intensity was decreased over the length of the tapered diffuser by the factor $m(l)$ shown in Equation 1, with l being the position along the diffuser axis and L being the maximal diffuser length. For the cylindrical diffuser, $m = 1$, hence, the surface brightness distribution on the diffuser corresponds to the power profile distributed to the surrounding volume.

$$m(l) = \left(1 - \frac{l}{L}\right) \quad (1)$$

Two different simulation methods were applied: a two-dimensional Monte Carlo simulation approach performed with Matlab (R2018a, The MathWorks, Natick, MA, USA) [14] and a three-dimensional approach using the ray tracing software LightTools (Version 8.5, Synopsys, Mountain View, CA, USA). For both simulation approaches a total of 1×10^7 rays were modelled.

For the Matlab approach, the intersection points between photon and shape of the diffuser were calculated using a Newton Algorithm [19]. Therefore, the photon path and the diffuser shape were expressed as mathematical equation of a straight line in the following form:

$$y(x) = kx + t \quad (2)$$

where:

k is the slope of the straight line

t is the ordinate intercept of the straight line.

The location of photon generation t_p is a number between $\pm r_{\text{core}}$ randomly generated by an internal Matlab

command, hence generating only photons within the fiber core. The value of k_p depends on the photon emission angle β , which was also generated randomly between $\pm \beta_{\max}$. The value for k_p can be calculated according to Equation 3.

$$k_p = \tan(\beta_{\max}) \quad (3)$$

If a photon hits the surface of the fiber, it either decouples or gets reflected. This is described by a decoupling probability p , which was set to $p = 0.815$, according to previous studies [15].

In case the photon is reflected within the fiber core, the sign of k_p changes and a new ordinate intercept has to be calculated:

$$t_p = y_{\text{ref}} - k_p x_{\text{ref}} \quad (4)$$

where:

y_{ref} is the y-value of the intersection point

x_{ref} is the x-value of the intersection point

The ordinate intercept of the shape t_s represents the radius of the diffuser, which can be modified in order to fit to the real diffuser shape. If the shape is cylindrically, the value of k_p was set to $k_p = 0$. If the shape is tapered, k_p can be calculated according to Equation 5.

$$k_p = -t_s l \quad (5)$$

where:

l is the length of the diffuser

The intersection point of y_s and y_p is calculated by using the Newton Algorithm. Therefore, Equation 6 was minimized to $f \rightarrow 0$.

$$f = y_s^2 - y_p^2 \quad (6)$$

where:

y_s is the path function of the shape

y_p is the path function of the photon

For the LightTools simulation a fiber with the implemented diffusers, the cladding, the light source and the receivers were modeled. The fiber core was set to a cylinder with a diameter of 600 μm and a length of 1.5 m. The core was surrounded by a tube with an inner diameter of 600 μm and a thickness of 15 μm , which acted as cladding. The refractive indices were set according to the optical properties of the processed fibers to $n_{\text{core}} = 1.46$ for the core and $n_{\text{cladding}} = 1.37$ for the cladding material. Hence, the angle of total internal reflection can be calculated according to Equation 7. Therefore, rays with an incident angle smaller than $\pm \beta_{\max}$ will be guided inside the fiber core.

$$\theta_c = \sin^{-1} \left(\frac{n_{\text{cladding}}}{n_{\text{core}}} \right) = \sin^{-1} \left(\frac{1.37}{1.46} \right) = 69.77^\circ$$

$$\beta_{\max} = 90^\circ - \theta_c = 20.23^\circ \quad (7)$$

The laser machined surfaces were modeled as lambertian scattering surfaces.

To model a light source, a circular surface emitter ($d = 590 \mu\text{m}$) was placed at the proximal fiber end. The source emitted rays with a random angle in the range of $\pm\beta_{max}$.

To detect photons decoupled from the diffuser surface, surface receivers (red) were placed around the diffusing area, as shown in Fig. 4. The surface receivers were attached to the inner surfaces of a hollow cuboid. The inner dimension of the cuboid were $630 \mu\text{m} \times 630 \mu\text{m}$ and a length of 30 mm with absorbing surfaces. The diffuser was placed in the middle of the cuboid.

In order to compare the measured radiation profiles of the tapered and the cylindrical diffuser, both profiles were visualized in one graph. This was performed for the surface brightness along the diffuser length as well as the distributed power to the surrounding volume. By adding the radiation profiles obtained by simulations, a comparison between measurement and simulation for the tapered and the cylindrical diffuser tip was performed.

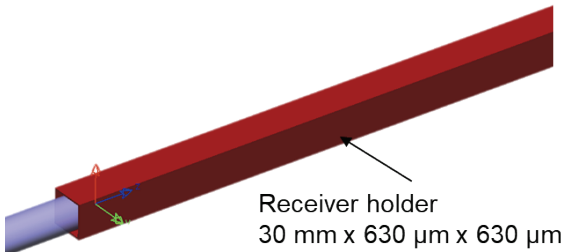


Fig. 4 Model used in LightTools simulation. Processed fiber core (blue) and receiver surfaces (red).

3. Results

In Fig. 5 the measured surface brightness on the diffuser is shown for a tapered (black) and a cylindrical (red) fiber tip. While the intensity of the cylindrical diffuser decays over the full diffuser length, the tapered form leads to an emission with almost constant intensity over the complete diffuser length.

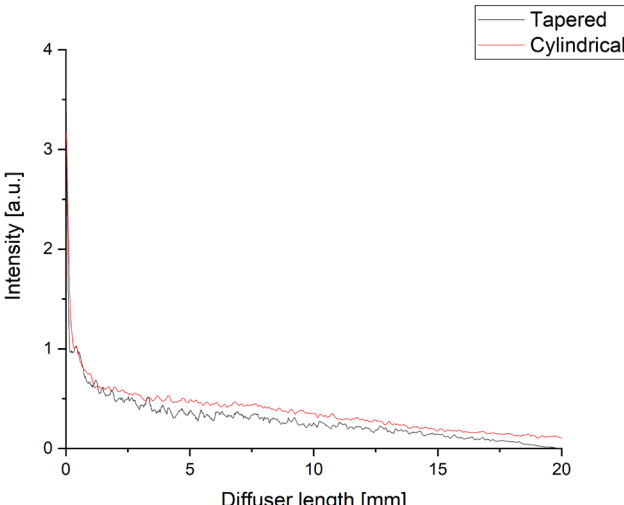


Fig. 5 Brightness on the surface of a tapered (black) and cylindrical (red) diffuser measured with camera setup.

In Fig. 6 the power distributions to the surrounding volume are shown for the tapered and the cylindrical diffuser. A strong emission at the diffuser beginning (diffuser length = 0 mm) and a fast decrease in intensity can be seen for both geometries within the first 2 mm. After approximately 2 mm both emission intensities have a constant decrease over the remaining diffuser length.

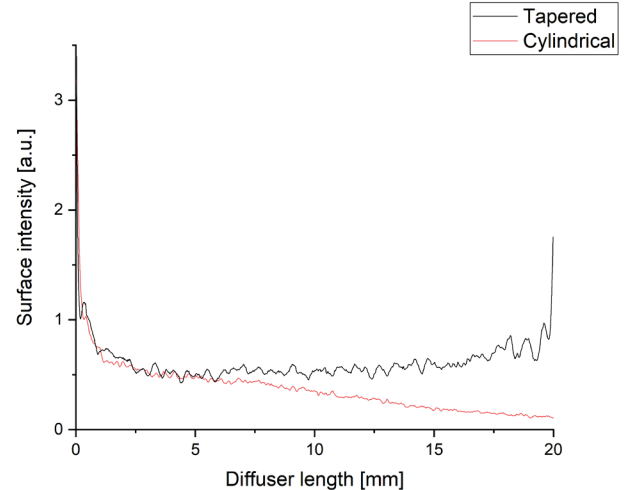


Fig. 6 Radiation profile of tapered (black) and cylindrical (red) shaped diffuser measured with camera setup.

The emission profiles gained from the Matlab and the LightTools simulations are shown in Fig. 7 and 8 for the tapered and the cylindrical diffuser tip respectively. For better comparison, also the measured emission profiles shown in Fig. 6 are added to both Figures. The tapered and the cylindrical geometry show an equivalent behaviour in its radiation profile for both simulative approaches. At the starting point of the laser ablated area (diffuser length = 0 mm), a strong emission can be detected, followed by a region of constant radiation with a length of approximately 2.5 mm for the LightTools simulation and 2 mm for the Matlab simulation. Afterwards, the simulated intensity drops in approximately 3 mm to almost zero emission, where the LightTools simulation decreases faster than the Matlab one's. Hence, most of the photons are decoupled within approximately 7 mm of diffuser length.

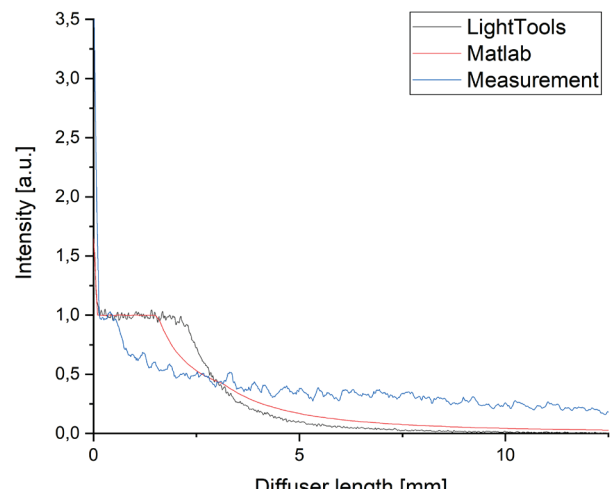


Fig. 7 Radiation profile of tapered shaped diffuser simulated with Matlab (red) and LightTools (black).

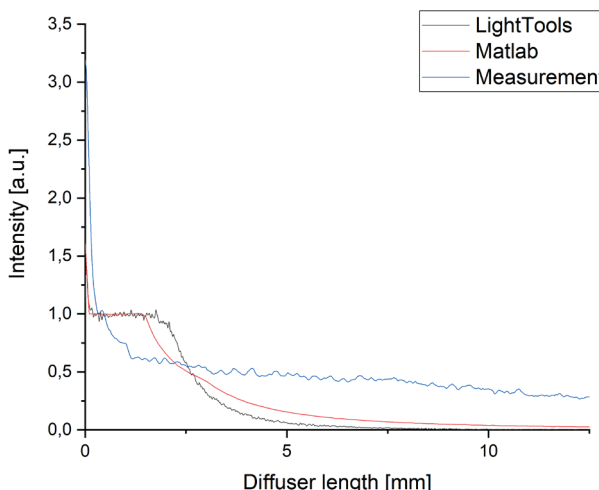


Fig. 8 Radiation profile of cylindrically shaped diffuser simulated with Matlab (red) and LightTools (black).

4. Discussion

The aim of the presented investigation was to develop a method to manufacture radially emitting diffusers by means of ultrafast-laser surface ablation of the fiber material for use in medical application. By setting the angular shift of the rotational axis to 9°, one tapered and one cylindrical diffuser was fabricated. The brightness on the diffuser surface (surface brightness over diffuser length) was measured by a camera imaging setup. From the surface brightness, the irradiated power distribution to the surrounding tissue was calculated and compared to intensity profiles simulated via Matlab (Monte Carlo) and Light Tools (Ray tracing).

Regarding the comparison of the emitted power between cylindrical and tapered shaped diffusers, no differences concerning the emission profiles were observed. This may be explained by the fact, that the emitted power isn't affected by the reduction in diffuser diameter along the diffuser length. However, observing the intensity on the diffuser surface, the cylindrical diffuser showed a decreasing emission profile, whereas the tapered one showed a constant intensity emission over the complete diffuser length. This could be of interest for high power applications, where tissue coagulation is not desired directly on the transition between diffuser and tissue. For low power applications, such as PDT, a homogeneous power distribution within the tissue is desired.

Comparing the measurement results to the results gained from the simulation, major differences could be observed. The area of constant emission in the simulation can be connected to the maximal photon angle $\pm \beta_{max}$. The length of the constant area can be calculated via $l_{const} = d_{core} \tan(\beta_{max})$. After l_{const} the first photons (emission angle $\pm \beta_{max}$) intersect with the diffuser surface for a second time. As a fraction of the photons with this emission angle have already decoupled at the first intersection, the emitted intensity starts to decay. However, the region of constant emission is not visible in the measured data set. The second difference between measurement and simulation is the decay after the region of constant emission. While the manufactured diffusers emit over the whole processed

length, the simulated diffuser models decouple most photons within approximately 7 mm.

These differences might be attributed to the used measurement method. As the field of view of a camera-lens system is limited by the acceptance angle of the lens, emitted rays above a certain angle might not be detected. Future work should therefore target towards a comparison between different measurement techniques to find a method modelling the light emission distribution most correctly.

The mismatch could also be caused by the limitations and simplifications performed in the simulations with regard to the decoupling probability. As the decoupling probability coefficient was determined by transmission measurements [15], it has to be investigated, whether it can form the basis for the performed simulations. Part of the decoupling is potentially related to the surface roughness. Therefore, the simulation have to be remodeled to consider the influence of surface roughness on the decoupling process. As the surface roughness of ultrafast-laser machined surfaces is tunable by varying the laser parameter [16], roughness could be used to further customize the radiation profile.

A major drawback of the production mechanism is the poor mechanical stability of the manufactured fiber diffusers. Upon completion the fiber tips are very sensitive for bending and mechanical input. This limits the application in a medical environment as the flexibility and stability of the light guide and its tip is crucial. A possible solution might be to recoat the processed fiber tip with a non-absorbing but scattering material. Thereby, it may be possible to restore the initial mechanical fiber conditions. Whether this acts as an applicable solution and how a potential recoating might affect the radiation profile has to be part of further investigations.

Compared to other fabrication techniques of fiber-based diffusers, the presented approach comprises several advantages. By using an ultrafast-laser system ($\lambda = 520$ nm) a twenty times higher precision can be reached compared to CO₂ laser ($\lambda = 10,600$ nm) processing, as the emission wavelength is 20 times smaller. Therefore, a tighter focus can be reached. While deploying internal refractive index changes by the use of an ultrafast-laser guarantees a high mechanical stability after fiber processing, a reproducible manufacturing process is difficult to establish, as defects in the cladding or dirt on the fiber surface may lead to a shift in the focus position. This strongly influences the manufacturing outcome, as the Rayleigh length is in the range of 1 μm to 10 μm. Performing surface ablation, the Rayleigh length of the beam can be increased to a few 100 μm by the use of a long-focal-length objective, allowing a reproducible processing.

By continuing the development of radially emitting fiber-based diffusers several applications can profit. Next to a patient specific diffuser, which guarantees a full illumination of the targeted tissue volume for PDT, also high power applications in laser-induced thermotherapy (LITT) [20] or endovenous laser treatment (EVLT) [6] could be targeted. Detaching from the clinical field, diffusers can be used for other lighting solutions, such as buildings, cars, displays [21], or even manufacturing light emitting textile samples [22].

5. Conclusion

In this work the radiation profile of tapered and cylindrical diffusers were measured and simulated. It was shown that tapered diffuser tips have a constant light emission on the diffuser surface, however, with continuously decreasing power distribution within the surrounding volume. By further improving the simulation models, as well as the measurement technique, the decoupling process could be better understood, which may lead to the development of diffusers with application specific radiation profiles.

Acknowledgements

Thanks to all colleagues at the research center for microtechnology at the Vorarlberg University of Applied Sciences for the technical support and the interesting discussions. The financial support by the Austrian Federal Ministry of Science, Research and Economy and the National Foundation for Research, Technology and Development is gratefully acknowledged. Part of this work was funded by the "Austrian Bridge-Program" (project "GlaDiLas" no. 855657) via the Austrian Research Promotion Agency (FFG).

This manuscript is part of the inaugural thesis of Stephan Ströbl to be submitted at the Medical Faculty of the Ludwig-Maximilians-Universität, Munich.

References

- [1] D. Dolmans, D. Fukumura, and R. K. Jain: Nat. Rev. Cancer, 3, (2003) 380.
- [2] A. P. Castano, T. N. Demidova, and M. R. Hamblin: Photodiagn. Photodyn., 1, (2004) 279.
- [3] A. P. Castano, T. N. Demidova, and M. R. Hamblin: Photodiagn. Photodyn., 2, (2005) 1.
- [4] T. J. Beck, F. W. Kreth, W. Beyer, J. H. Mehrkens, A. Obermeier, H. Stepp, W. Stummer, and R. Baumgartner: Laser Surg. Med., 39, (2007) 386.
- [5] A. Rühm, H. Stepp, W. Beyer, G. Hennig, T. Pongratz, R. Sroka, O. Schnell, J. C. Tonn, and F. W. Kreth: Proc. SPIE BiOS, 8928, (2014) 13.
- [6] R. Sroka, H. Stepp, G. Hennig, G. M. Brittenham, A. Rühm, and L. Lilge: J. Biomed. Opt., 20, (2015) 061110.
- [7] T. M. Baran, and T. H. Foster: Med. Phys., 41, (2014) 022701.
- [8] L. H. P. Murrer, J. P. A. Marijnissen, and W. M. Star: Phys. Med. Biol., 41, (1996) 951.
- [9] E. U. Simsek, B. Simsek, and B. Ortac: Appl. Phys. B, 123, (2017) 176.
- [10] T. H. Nguyen, Y. H. Rhee, J. C. Ahn, and H. W. Kang: Opt. Express, 23, (2015) 20829.
- [11] V. V. Volkov, and V. B. Loshchenov: Quantum Electron., 40, (2010) 746.
- [12] J. Köcher, V. Knappe, and M. Schwagmeier: Photonics Lasers Med., 5, (2015) 57.
- [13] D. Ashkenasi, A. Rosenfeld, S. B. Spaniol, and A. Terenji: Proc. SPIE, 4978, (2003) 180.
- [14] H. Varel, D. Ashkenasi, A. Rosenfeld, M. Wähmer, and E. E. B. Campbell: Appl. Phys. A, 65, (1997) 367.
- [15] M. Domke, J. Gratt, and R. Sroka: Proc. SPIE, 9740, (2016) 22.
- [16] D. Lambelet, Y. Bellouard, and C.-A. Ranély-Vergé-Dépré: Proc. SPIE, 10522, (2018) 20.
- [17] J. Gratt: "Fabrication of optical fibre diffusers using fs-lasers", Master thesis Mechatronics, FH Vorarlberg, (2015).
- [18] B. Jaeggi, S. Remund, R. Streubel, B. Goekce, S. Barcikowski, and B. Neuenschwander: J. Laser Micro/Nanoengin., 12, (2017) 267.
- [19] T. J. Ypma: Siam Rev., 37, (1995) 531.
- [20] V. Knappe, A. Roggan, M. Glotz, M. Müller, J. P. Ritz, C. T. Germer, and G. Müller: Med. Laser Appl., 16, (2001) 73.
- [21] Y. Okuda, K. Onoda, and R. Fujieda: Opt. Eng., 51, (2001) 074001.
- [22] T. Khan, M. Unternährer, J. Buchholz, B. Kaser-Hotz, B. Selm, M. Rothmaier, and H. Walt: Photodiagn. Photodyn., 3, (2006) 51.

(Received: June 12, 2018, Accepted: February 2, 2019)